Proc. Natl. Acad. Sci. USA
Vol. 85, pp. 2398-2402, April 1988
Neurobiology

Spatial distribution of calcium channels and cytosolic calcium transients in growth cones and cell bodies of sympathetic neurons

(single channel/patch clamp/fura-2/digital imaging/calcium stores)

DIANE LIPSCOMBE*, DANIEL V. MADISON*, MARTIN POENIE†‡, HARALD REUTER*§, ROGER Y. TSIEN†, AND RICHARD W. TSIEN*

*Department of Cellular and Molecular Physiology, Yale University School of Medicine, New Haven, CT 06510; and †Department of Physiology–Anatomy, University of California, Berkeley, CA 94720

Communicated by Joseph F. Hoffman, November 18, 1987 (received for review July 28, 1987)

ABSTRACT **Ca^{2+} imaging and single-channel recording were used to study the regulation of cytosolic free Ca^{2+} ($[Ca^{2+}]_i$) in local regions of frog sympathetic neurons. Digital imaging with the fluorescent Ca^{2+} indicator fura-2 demonstrated: (*i*) resting $[Ca^{2+}]_i$ of 70–100 nM; (*ii*) significant increases in $[Ca^{2+}]_i$ in growth cones and cell bodies following depolarization induced by extracellular electrical stimulation or increased external K^+; (*iii*) in cell bodies, large transient increases in $[Ca^{2+}]_i$ following exposure to caffeine and sustained oscillations in $[Ca^{2+}]_i$ in the presence of elevated K^+ and caffeine; and (*iv*) in growth cones, smaller and briefer changes in $[Ca^{2+}]_i$ in response to caffeine. The nature of the depolarization-induced Ca^{2+} entry was studied with cell-attached patch recordings (110 mM Ba^{2+} in recording pipette). Ca^{2+} channel activity was observed in 18 of 20 patches on cell bodies, 3 of 5 patches along neurites, and 36 of 41 patch recordings from growth cones. We observed two types of Ca^{2+} channels: L-type channels, characterized by a 28-pS slope conductance, sensitivity to dihydropyridine Ca^{2+} channel agonist, and availability even with depolarizing holding potentials; and N-type channels, characterized by a 15-pS slope conductance, resistance to dihydropyridines, and inactivation with depolarized holding potentials. Both types of channels were found on growth cones and along neurites as well as on cell bodies; channels often appeared concentrated in local hot spots, sometimes dominated by one channel type.**

Specialized regions of neurons undergo localized changes in intracellular calcium concentration ($[Ca^{2+}]_i$) that are important in controlling excitability (1), transmitter release (2, 3), and neurite extension (4–6). However, compared to information about Ca^{2+} mobilization in neuronal cell bodies (e.g., ref. 7), relatively little is known about the mechanisms for Ca^{2+} delivery and uptake in dendrites, synaptic terminals, and growth cones (8). Growth cones are particularly interesting because their dynamic activity determines the pattern of connection between neurons and target cells (9, 10); they release neurotransmitters, as do synaptic terminals (11–13), and thus provide a model system for studying synaptic function. Some evidence has been provided for Ca^{2+} channels in growth cones of certain cells (14–16) but not others (17). To study intracellular Ca^{2+} regulation in growth cones, neurites, and cell bodies of frog sympathetic neurons, we have used two complementary approaches: imaging of $[Ca^{2+}]_i$ with the fluorescent Ca^{2+} indicator dye fura-2 (18) and cell-attached patch clamp recordings (19). Fura-2 imaging allowed us to detect local changes in $[Ca^{2+}]_i$ resulting from Ca^{2+} entry through voltage-gated Ca^{2+} channels or Ca^{2+} release from intracellular stores and to monitor oscillations in $[Ca^{2+}]_i$. Patch clamp recordings revealed the coexistence of N-type and L-type Ca^{2+} channels on the surface of growth cones and along neurites, like those found on cell bodies (refs. 20 and 21; cf. refs. 22 and 23). A preliminary account of this data has been presented (24).

MATERIALS AND METHODS

Preparation of Cells. Paravertebral ganglia were removed from frogs (*Rana pipiens*) and incubated at room temperature for 45 to 60 min in a modified Ringer's solution containing 120 mM NaCl, 5 mM KCl, 10 mM glucose, 10 μM $CaCl_2$, and 5 mM Hepes (pH 7.4 with NaOH), with 0.3% collagenase added. Ganglia were triturated to remove loose connective tissue, transferred to a solution containing 0.15% trypsin for ≈10 min, thoroughly rinsed in enzyme-free solution, and dissociated by trituration (25). Dissociated cells were concentrated by centrifugation, resuspended in culture medium [75% (vol/vol) L-15 (GIBCO), 10% (vol/vol) fetal bovine serum, penicillin at 50 units/ml, streptomycin at 50 μg/ml, 4 mM $CaCl_2$, 5 mM Hepes (pH 7.4)], plated onto culture dishes for electrophysiology or poly(lysine)-coated glass coverslips for imaging, and kept at room temperature for up to 5 days. Neurites were first observed on day 2 following dissociation. Their growth rate was slow (≈1 μm/hr) and sporadic, conditions that did not favor observing the large $[Ca^{2+}]_i$ gradients between growth cones and cell bodies reported by Connor (16) in rapidly growing processes of mammalian neurons. The small gradients that we did observe (see *Results*) were sometimes but not always abolished by removing external Ca^{2+}.

Electrophysiological Recordings. Unitary Ca^{2+} channel currents were recorded from cell-attached patches (19), filtered at 1 kHz (−3 dB; 8 pole Bessel), digitized at 5 kHz, and stored in a computer. Recording pipettes were filled with a solution containing 110 mM $BaCl_2$, 0.2–1 μM tetrodotoxin, and 5 mM Hepes (pH 7.4) and had resistances of 2–5 MΩ. The bathing solution contained 140 mM potassium aspartate, 10 mM EGTA, and 10 mM Hepes (pH 7.4) and zeroed the membrane potential of the cell. The dihydropyridine agonist (+)-(*S*)-202-791 (Sandoz) was often added to the external solution to prolong L-type Ca^{2+} channel openings (26).

Fura-2 Imaging of $[Ca^{2+}]_i$. Neurons were loaded with fura-2 in a mixture of 2 ml of modified Ringer's solution and of 1–5 μl of a solution containing 1 mM fura-2 acetoxymethyl ester (Molecular Probes, Junction City, OR) and 25% (wt/wt) Pluronic F-127 (BASF Wyandotte, Wyandotte, MI) in dimethyl sulfoxide (final concentration of fura-2 acetoxy-

The publication costs of this article were defrayed in part by page charge payment. This article must therefore be hereby marked "*advertisement*" in accordance with 18 U.S.C. §1734 solely to indicate this fact.

Abbreviation: $[Ca^{2+}]_i$, cytosolic free Ca^{2+} concentration.

‡Present address: Department of Zoology, University of Texas, Austin, TX 78713.
§Present address: Department of Pharmacology, University of Bern, Bern, CH-3010 Switzerland.

methyl ester between 0.5 and 2.5 μM). After gentle agitation in the loading solution for 30 to 40 min (≈22°C), cells were transferred to dye-free Ringer's solution and used shortly after rinsing. The intracellular fura-2 concentration was estimated as 50–100 μM based on comparison of the mean brightness of cells with that of a few cells in which fura-2 free-acid was introduced through a patch pipette in whole-cell mode. Completeness of deesterification was checked by addition of ionomycin at normal extracellular [Ca^{2+}] and verification that the fura-2 350-nm/385-nm excitation ratio was more than 12 times that for fura-2 in EGTA.

For imaging experiments, dye-loaded cells with diffuse fluorescence lacking visible dye compartmentation were selected for study in most cases. Trapping of dye in organelles cannot be ruled out completely, although exposure of cells to digitonin to permeabilize the surface membrane generally caused a rapid disappearance of fluorescence. Cell autofluorescence, which would not be subtracted by this procedure, appeared negligible at the usual gain settings, though a little could be detected in nonloaded cells at increased camera gain. Cells were bathed in modified Ringer's solution containing 2 mM $CaCl_2$. For high K^+ solutions, KCl was substituted for NaCl. Control experiments demonstrated that complete replacement of NaCl by LiCl caused no change in basal $[Ca^{2+}]_i$. New solutions were applied within 1 s by removing old solution by suction and adding new solution by pipette. Drugs were removed by a series of two or three such solution changes within a few seconds. All experiments were carried out at room temperature (≈22°C).

Fluorescence digital imaging was used to determine the spatial distribution of $[Ca^{2+}]_i$ (27) as detailed elsewhere (28). Briefly, fluorescence images were taken with excitation at either 350 nm or 385 nm and emission-filtered with a 418-nm long pass filter. After subtraction of background images, obtained from an adjacent cell-free portion of the chamber, the ratio of fluorescent intensities at the two wavelengths was calculated pixel by pixel and converted into a display of Ca^{2+} concentration by means of a calibration curve (18) in which $K_d S_{f2}/S_{b2}$ was taken as 1.8 μM. This method effectively normalizes for differences in cell thickness and dye concentration (29). Fluorescent images were collected with a low-light-level camera (Dage-MTI, Michigan City, IN) connected to the camera port of an inverted microscope equipped with a Nikon ×40 objective lens (UV-F series; 1.3 numerical aperature; glycerin). The camera output was analyzed by a digital image processor (model FD5000; Gould Imaging and Graphics, Fremont, CA) under control of a PDP 11/73 computer (Digital Equipment, Maynard, MA). In a typical experiment, 32 images were taken at each excitation wavelength for averaging before the calculation of the ratio image. The time resolution of the measurements was ≈2 s. Images are shown on a pseudocolor display where color indicates $[Ca^{2+}]_i$ levels, and brightness indicates the overall fluorescent intensity.

RESULTS

Fura-2 imaging was used to examine the spatial distribution of $[Ca^{2+}]_i$ in cultured sympathetic neurons that had developed neurites ending in growth cones. The average resting $[Ca^{2+}]_i$ in the cell body was 79 ± 14 nM (mean ± SEM, 11 cells). In 16 growth cones of the same group of cells, $[Ca^{2+}]_i$ averaged 131 ± 20 nM. These values are similar to those reported in rat central nervous system neurons (13) for cell bodies (60–80 nM) and growth cones undergoing random movement or slow outgrowth (70–200 nM).

$[Ca^{2+}]_i$ Distribution During Depolarization. The response of $[Ca^{2+}]_i$ to changes in membrane potential was studied in neurons depolarized by elevating external K^+ (Fig. 1 *A–C*) or by electrical stimulation (Fig. 1 *D–F*). Depolarization evoked a large increase in $[Ca^{2+}]_i$ that was abolished by removing external Ca^{2+}, consistent with Ca^{2+} entry via voltage-activated Ca^{2+} channels. The depolarization-induced increase in $[Ca^{2+}]_i$ was much the same in all regions of the cell. For example, exposure to 60 mM K^+ evoked an increase in $[Ca^{2+}]_i$ of 231 ± 35 nM in cell bodies (six neurons) compared to 216 ± 59 nM in growth cones of the same cells. Similar responses in growth cones and cell bodies were also seen with electrical stimulation (Fig. 1 *D–F*).

Type and Overall Distribution of Ca^{2+} Channels. The rapid and uniform increase in Ca^{2+} levels suggested that voltage-gated Ca^{2+} channels are present in all regions of the cell. To test this hypothesis, we made cell-attached patch recordings from soma, neurites, and growth cones of sympathetic neurons with pipettes containing 110 mM Ba^{2+}. Ca^{2+} channel activity was observed in 18 of 20 patches on cell bodies, 3 of 5 patches along neurites, and 36 of 41 patch recordings from growth cones.

Analysis of these recordings revealed two types of Ca^{2+} channels with properties similar to N- and L-type channels of chicken dorsal root ganglion neurons (22, 23) and rat

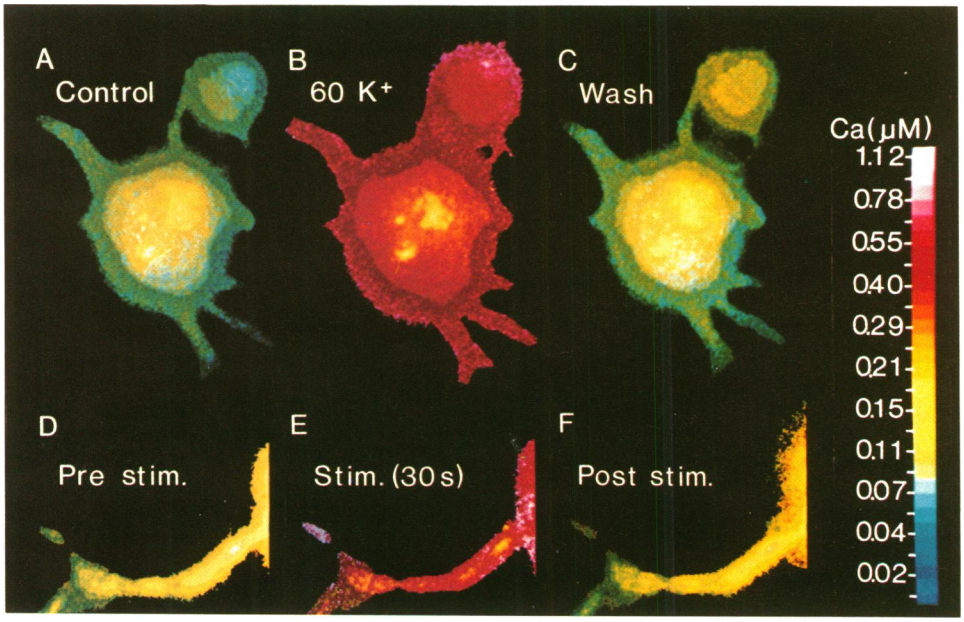

FIG. 1. Changes in $[Ca^{2+}]_i$ in response to depolarizing stimuli detected with digital imaging of fura-2. (*A–C*) Images of a neuron with four processes (lower cell) and a smaller neuron (upper cell). Distribution of $[Ca^{2+}]_i$ in cells in 5 mM K^+ (*A*), 11 s after depolarization by exposure to 60 mM K^+ (*B*), and after a 260-s recovery in normal Ringer's solution (*C*). The unresponsive patches in the cell center are due to overload of the dynamic range of the camera or of the analog-to-digital converter. (*D–F*) Changes in $[Ca^{2+}]_i$ in a neurite in response to electrical stimulation with an extracellular microelectrode on the cell body (only a portion of the cell body is shown). Images before stimulation (*D*), after a train of stimuli (*E*, 1-ms pulses at 5 Hz for 30 s), and after a 35-s recovery (*F*).

sympathetic neurons (20). No T-type Ca^{2+} channels were detected (see also refs. 20 and 30). In frog sympathetic neurons as in other neurons, N- and L-type Ca^{2+} channels could be distinguished by their unitary conductance, voltage-dependence, and pharmacology (20, 22, 23). Fig. 2*A* shows a representative cell-attached patch recording from a cell body illustrating activity of both types of channels. Test depolarizations to −10 mV evoked clearly resolved openings of ≈0.8 pA and ≈1.8 pA, corresponding to slope conductances of 15 and 28 pS calculated from the current–voltage relationships (Fig. 2*B*), in good agreement with conductances of N- and L-type Ca^{2+} channels reported (20, 22, 23). As in other preparations, openings of the large conductance L-type channels were greatly prolonged by the dihydropyridine agonist (+)-(*S*)-202-791 (26), whereas the smaller N-type Ca^{2+} channel openings were unaffected (19). Both types of channels were activated with progressively stronger depolarizations over the range between −30 mV and +20 mV (Fig. 2*C*).

N- and L-type Ca^{2+} channels were also found on growth cones (Fig. 2*C*) and showed properties very similar to their counterparts on the cell body. There was no detectable difference between growth cones or cell bodies with respect to unitary amplitudes of N- or L-type openings (Fig. 2*B*).

Microscopic Distribution of Ca^{2+} Channels. In growth cones, as in cell bodies, openings of N- and L-type channels appeared together in some patches (Fig. 2*A*) and in near isolation in other patches (Fig. 4*A*). When found in the same patch, activity of N- and L-type Ca^{2+} channels was separated by virtue of their different inactivation properties (Fig. 3). N-type channels were available at negative holding potentials (e.g., −80 mV; Fig. 3 *Left*) and were largely, but not completely, inactivated at depolarized holding potentials (−40 mV; Fig. 3 *Right*). Activity of L-type channels was much more resistant to inactivation with steady depolarization and remained at a holding potential of −40 mV (20–23).

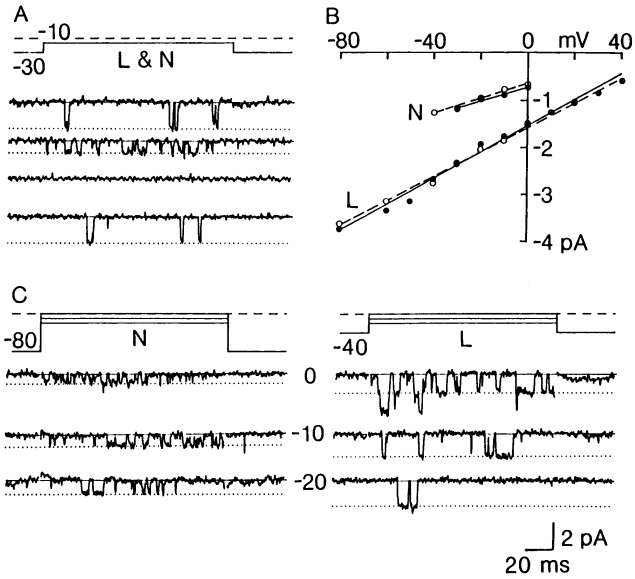

FIG. 2. Properties of L- and N-type Ca^{2+} channels in cell bodies and growth cones of sympathetic neurons. Unitary Ca^{2+} channel currents recorded from cell-attached patches with 110 mM $BaCl_2$ as the charge carrier in the recording pipette and 5 μM (+)-(*S*)-202-791 in the bathing solution. (*A*) Openings of L- and N-type Ca^{2+} channels from a patch on a neuron soma, elicited by the voltage protocol illustrated. Unitary currents carried by the L-type Ca^{2+} channel (≈2 pA) are about twice the amplitude of those of the N-type channel (≈1 pA). (*B*) Single-channel current amplitude plotted against membrane potential for L- and N-type channel openings recorded from cell bodies (open circles) and growth cones (solid circles). Linear regression analysis yielded slope conductances for cell bodies and growth cones of 26 pS (n = 12) and 28 pS (n = 7) for L-type channels and 16 pS (n = 8) and 15 pS (n = 6) for N-type channels. (*C*) Recordings from two growth cone patches showing the voltage dependence of single-channel currents carried by L- and N-type Ca^{2+} channels. Dotted lines indicate average current amplitudes determined by measurement of several individual openings at each test potential.

Hot spots of Ca^{2+} channel activity were found in about half of the recordings from growth cones or cell bodies; sometimes one type of Ca^{2+} channel activity prevailed (Fig. 4). A predominance of N-type channels is evident in Fig. 4*A* since channel activity was almost completely inactivated at a holding potential of −30 mV; in contrast, a patch rich in L-type channel activity (Fig. 4*B*) shows little inactivation at a holding potential of −30 mV. Varying the level of the test pulse demonstrates that N-type channel activation becomes significant at test potentials slightly more negative than those required by L-type channel activation (Fig. 4*B*). Thus, N- and L-type Ca^{2+} channels can be distinguished at the level of individual openings or many openings dominated by one or other channel type. Both types of Ca^{2+} channels are found in all regions of the neuron, but there may be microscopic heterogeneity in their spatial distribution.

Intracellular Ca^{2+} Stores. To study the functional contribution of Ca^{2+} stores in various regions of the neuron, we applied caffeine, an agent known to promote Ca^{2+} release in neurons (31, 32). Fig. 5 shows a cell body with a prominent growth cone. Changes in $[Ca^{2+}]_i$ induced by 60 mM K^+ or 10 mM caffeine are illustrated with selected images (Fig. 5*A*) or time plots for specific regions of the cell (Fig. 5 *B* and *C*). Whereas depolarization with 60 mM K^+ induced similar increases in $[Ca^{2+}]_i$ in the cell body and in the growth cone, caffeine evoked a pronounced $[Ca^{2+}]_i$ response in the cell body but little response in the growth cone. Regional differences between the caffeine response in cell bodies and growth cones were not always so extreme. In some experi-

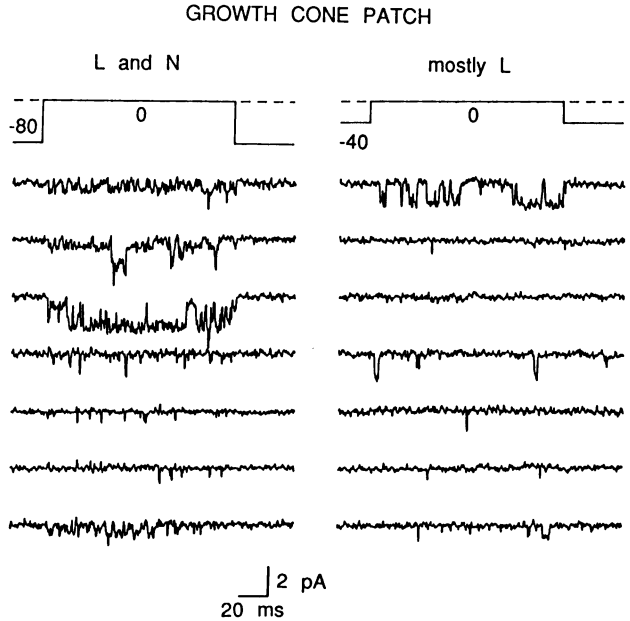

FIG. 3. L-type and N-type Ca^{2+} channels distinguished by their dependence on holding potential. Current records from a cell-attached patch on a growth cone are shown below the associated voltage protocols. Consecutive sweeps are in each column. From a holding potential of −80 mV (*Left*), voltage steps to 0 mV evoke unitary currents of two amplitudes corresponding to L- and N-type Ca^{2+} channels. With a holding potential of −40 mV (*Right*), test pulses to 0 mV evoke L-type Ca^{2+} channel openings almost exclusively. (+)-(*S*)-202-791 at 5 μM was in the bathing solution.

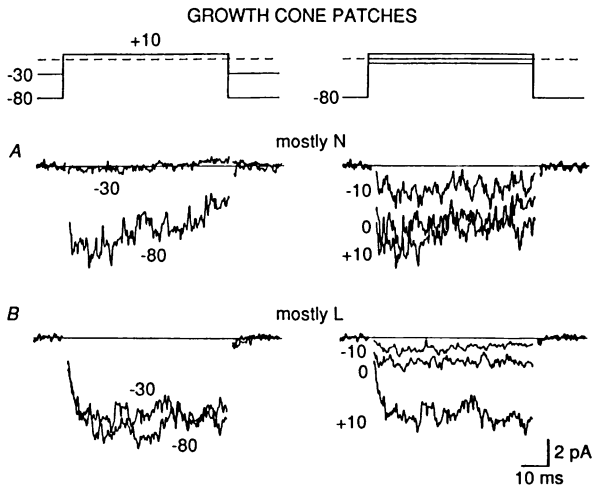

FIG. 4. Hot spots enriched in a particular type of Ca^{2+} channel, distinguished by their inactivation and activation properties. Cell-attached patch recordings from two growth cones containing several N-type Ca^{2+} channels (*A*) or several L-type Ca^{2+} channels (*B*). No dihydropyridine was present. Records are averages of three to six individual sweeps. At the left are current records showing the degree of inactivation produced by variations in the holding potential. In *A*, the patch contained mostly N-type channels since the slowly decaying current evoked from a holding potential of −80 mV was virtually inactivated at a holding potential of −30 mV. In *B*, a predominance of L-type Ca^{2+} channels is indicated since the sustained current evoked from a holding potential of −80 mV was hardly affected by changing the holding potential to −30 mV. At the right is the voltage dependence of activation. Currents in the patch containing mostly N-type Ca^{2+} channels (*A*) were activated at slightly more negative test levels than currents in the patch containing mostly L-type Ca^{2+} channels (*B*). This is a characteristic of N- and L-type Ca^{2+} channels with 110 mM external $BaCl_2$.

ments (e.g., Fig. 6), caffeine did produce a transient rise in $[Ca^{2+}]_i$ in the growth cone, though the response was always smaller and briefer than in the cell body. Quantitative differences were consistent (six experiments): caffeine increased $[Ca^{2+}]_i$ by 252 ± 32 nM in cell bodies (an elevation similar to that induced by 60 mM K^+ in the same cells) and by only 126 ± 40 nM in growth cones. The caffeine-induced Ca^{2+} transient in growth cones is compatible with caffeine-induced transmitter release from rat brain growth cones (33).

Further differences between Ca^{2+} mobilization in cell bodies and growth cones were observed when K^+ was elevated in the presence of caffeine (Fig. 6). The cell body displayed a K^+-induced increase in $[Ca^{2+}]_i$ that gave way to a sustained series of oscillations of $[Ca^{2+}]_i$. Such oscillations were not usually seen when caffeine or elevated K^+ were applied separately but were observed consistently when the stimuli were combined (three cells). In contrast to the cell body the growth cone responded to caffeine and high K^+ with an increase in $[Ca^{2+}]_i$ that declined slowly with little or no oscillatory activity (Fig. 6).

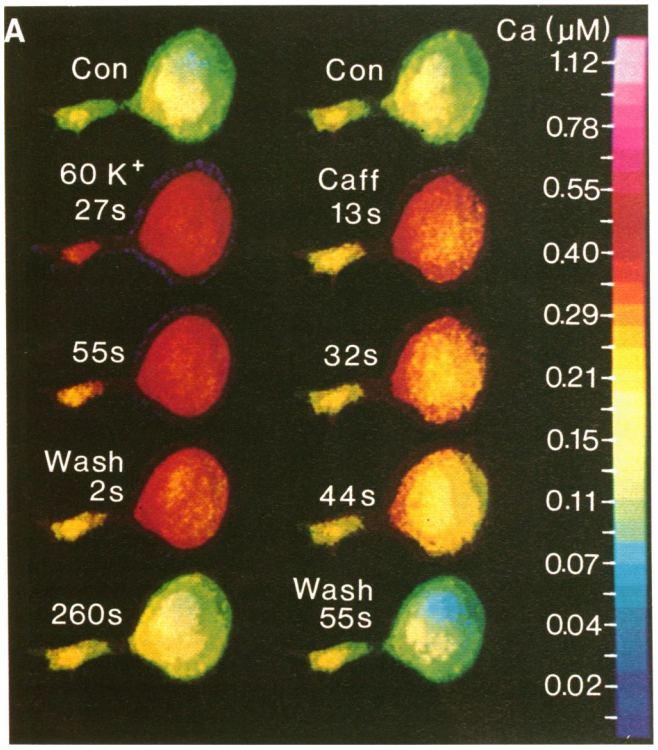

FIG. 5. Changes in $[Ca^{2+}]_i$ in response to 60 mM K^+ and 10 mM caffeine in the growth cone and cell body of a sympathetic neuron (*A*). Ratio images of $[Ca^{2+}]_i$ (*B*) and corresponding plot of $[Ca^{2+}]_i$ against time (*C*). Individual values for the growth cone and the cell body were obtained by spatial averaging over circular zones within the appropriate region of the image.

DISCUSSION

Fura-2 imaging and patch clamp recordings provided complementary information about the regulation of intracellular Ca^{2+} in various regions of sympathetic neurons. The imaging experiments gave a spatially resolved overview of $[Ca^{2+}]_i$ regulation in all parts of the neuron; they support the hypothesis that voltage-gated Ca^{2+} channels are present in all regions of neurons (8, 14, 15, 34), while suggesting that Ca^{2+} release from intracellular stores is more obvious in the cell body than in growth cones. The imaging directly demonstrates caffeine-induced $[Ca^{2+}]_i$ oscillations (see also ref. 35), prominent in the cell body but not the growth cone, consistent with observations of Ca^{2+}-dependent rhythmic hyperpolarizations (31). The possibile involvement of Ca^{2+}-induced Ca^{2+} release in Ca^{2+} transients evoked by depolarization is considered in a separate paper (36).

Cell-attached patch recordings revealed N- and L-type Ca^{2+} channels on growth cones and neurites as well as cell bodies (see also refs. 6, 14, and 37). In all regions of the cell, the single channel properties of these channels are consistent with macroscopic current recordings (6, 21). N-type channels can be distinguished from L-type channels by their smaller unitary conductance, their sensitivity to inactivation

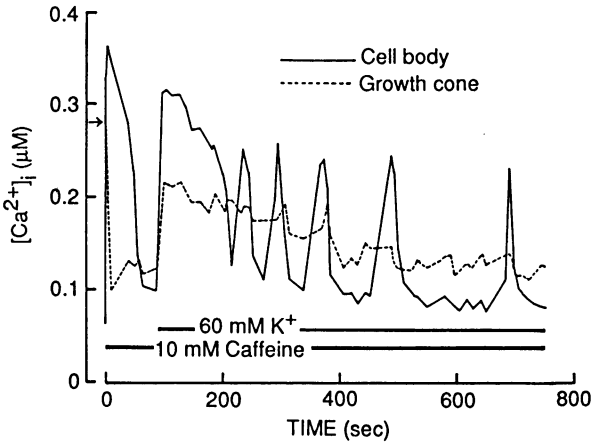

FIG. 6. Oscillations in $[Ca^{2+}]_i$ induced by the combined action of 10 mM caffeine and 60 mM K^+ in a growth cone and cell body. Addition of 10 mM caffeine induced a transient increase in Ca^{2+} in all regions of the neuron, the response in the cell body (solid trace) being larger and longer lasting than that in the growth cone (dashed trace) or along the neurite (data not shown). In the continued presence of caffeine, application of 60 mM K^+ induced an increase in $[Ca^{2+}]_i$ more sustained than the response to caffeine. Several seconds following application of 60 mM K^+, $[Ca^{2+}]_i$ levels in the soma went into rhythmic oscillations without further intervention. $[Ca^{2+}]_i$ levels in the growth cone declined gradually with little or no oscillation. Changes in $[Ca^{2+}]_i$ in the neurite were intermediate between those in the other two regions (analysis not shown).

by depolarized holding potentials, and their resistance to dihydropyridines. Finding N- and L-type channels on the cell body suggests that Ca^{2+} channels are not restricted to peripheral processes (see ref. 38) even in acutely dissociated adult neurons (21). Information about Ca^{2+} channels in growth cones is particularly interesting, because they are capable of evoked Ca-dependent release of neurotransmitters (11–13), as are synaptic terminals, that are difficult to study with direct electrical recordings. Finding N- and L-type Ca^{2+} channels on growth cones supports evidence in nerve terminals for channels that are dihydropyridine-insensitive (e.g., refs. 39–41) or sensitive (e.g., refs. 42–44). Although no gross differences were seen between the density of N- or L-type Ca^{2+} channels in growth cones and in other parts of the cell, we did find spatial heterogeneity on a smaller scale, in the form of hot spots sometimes dominated by either N- or L-type channels. Microscopic clusters of Ca^{2+} channels might be important if they were located near vesicular release mechanisms, enzymes, or other channels showing pronounced Ca-sensitivity. The available evidence, so far, suggests that N-type Ca^{2+} channels play a dominant role in mediating norepinephrine release from sympathetic neurons (20) and that L-type Ca^{2+} channels control substance P release from sensory neurons (45).

Regional differences in internal Ca^{2+} stores in neurons appeared in experiments studying caffeine-induced Ca^{2+} release. Growth cones displayed smaller and briefer changes in $[Ca^{2+}]_i$ than cell bodies when caffeine was applied individually or in combination with elevated K^+ (Figs. 5 and 6). This might be attributed to the cellular distribution of subsurface cisternae thought to mediate Ca^{2+} sequestration and release (46, 47); these structures are rare in growth cones (48) but abundant in cell bodies (46, 47, 49, 50). Another contributing factor may be a more rapid Ca^{2+} extrusion in growth cones because of their higher surface/volume ratio (8). Indeed, $[Ca^{2+}]_i$ levels recover somewhat more rapidly in growth cones than in cell bodies following removal of elevated K^+ (Fig. 5 *B* and *C*). Further work will be needed to determine the relative importance of these factors, but the results already demonstrate significant differences between Ca^{2+} regulation in specialized regions of neurons.

We thank Dr. C. F. Stevens for providing support for H.R. as a Visiting Professor. This work was supported by National Institutes of Health grants (to R.W.T. and R.Y.T.) and a Markey Fellowship (to D.V.M.).

1. Hagiwara, S. & Byerly, L. (1983) *Trends Neurosci.* **6**, 189–193.
2. Katz, B. & Miledi, R. (1971) *J. Physiol. (London)* **216**, 503–512.
3. Anglister, L., Farber, I. C., Shahar, A. & Grinvald, A. (1982) *Dev. Biol.* **94**, 351–365.
4. Suarez-Isla, B. A., Pelto, D. J., Thompson, J. M. & Rapoport, S. I. (1984) *Dev. Brain Res.* **14**, 263–270.
5. Cohan, C. S. & Kater, S. B. (1986) *Science* **232**, 1638–1640.
6. Streit, J. & Lux, H. D. (1987) *Pflügers Arch.* **408**, 634–641.
7. Tillotson, D. L. & Gorman, A. L. F. (1983) *Cell. Mol. Neurobiol.* **3**, 297–310.
8. Ross, W. N., Stockbridge, L. L. & Stockbridge, N. L. (1986) *J. Neurosci.* **6**, 1148–1159.
9. Lockerbie, R. O. (1987) *Neuroscience* **20**, 719–729.
10. Goodman, C. S., Bastiani, M. J., Doe, C. Q., duLac, S., Helfand, S. L., Kuwada, J. Y. & Thomas, J. B. (1984) *Science* **225**, 1271–1279.
11. Young, S. H. & Poo, M. (1983) *Nature (London)* **305**, 634–637.
12. Hume, R. I., Role, L. W. & Fischbach, G. D. (1983) *Nature (London)* **305**, 632–634.
13. Sun, Y. & Poo, M.-m. (1987) *Proc. Natl. Acad. Sci. USA* **84**, 2540–2544.
14. Grinvald, A. & Farber, I. A. (1981) *Science* **212**, 1164–1167.
15. Bolsover, S. R. & Spector, I. (1986) *J. Neurosci.* **6**, 1934–1940.
16. Connor, J. A. (1986) *Proc. Natl. Acad. Sci. USA* **83**, 6179–6138.
17. Belardetti, F., Schacher, S. & Siegelbaum, S. A. (1986) *J. Physiol. (London)* **374**, 298–313.
18. Grynkiewicz, G., Poenie, M. & Tsien, R. Y. (1985) *J. Biol. Chem.* **260**, 3440–3450.
19. Hamill, O. P., Marty, E., Neher, E., Sakmann, B. & Sigworth, F. J. (1981) *Pflügers Arch.* **391**, 85–100.
20. Hirning, L. D., Fox, A. P., McCleskey, E. W., Olivera, B. M., Thayer, S. A., Miller, R. J. & Tsien, R. W. (1988) *Science* **239**, 57–61.
21. Lipscombe, D. & Tsien, R. W. (1987) *J. Physiol (London)* **390**, 84P.
22. Nowycky, M. C., Fox, A. P. & Tsien, R. W. (1985) *Nature (London)* **316**, 440–443.
23. Fox, A. P., Nowycky, M. C. & Tsien, R. W. (1987) *J. Physiol. (London)* **394**, 173–200.
24. Lipscombe, D., Poenie, M., Reuter, H., Tsien, R. Y. & Tsien, R. W. (1986) *Biophys. J.* **51**, 227a (abstr.).
25. Lipscombe, D. (1986) Ph.D. Thesis (University of London, London).
26. Kokubun, S., Prod'hom, B., Becker, C., Porzig, H. & Reuter, H. (1986) *Mol. Pharmacol.* **30**, 571–584.
27. Williams, D. A., Fogart, K. E., Tsien, R. Y. & Fay, F. S. (1985) *Nature (London)* **318**, 558–561.
28. Poenie, M., Alderton, J., Steinhardt, R. & Tsien, R. (1986) *Science* **233**, 886–889.
29. Tsien, R. Y., Rink, T. J. & Poenie, M. (1985) *Cell Calcium* **6**, 145–157.
30. Marchetti, C., Carbone, E. & Lux, H. D. (1986) *Pflügers Arch.* **406**, 104–111.
31. Kuba, K. (1980) *J. Physiol. (London)* **298**, 251–269.
32. Neering, I. R. & McBurney, R. N. (1984) *Nature (London)* **309**, 158–160.
33. Lockerbie, R. O. & Gordon-Weeks, P. R. (1986) *Neuroscience* **17**, 1257–1266.
34. Ross, W. N. & Werman, R. (1987) *J. Physiol. (London)* **389**, 319–336.
35. Smith, S. J., MacDermott, A. B. & Weight, F. F. (1983) *Nature (London)* **304**, 350–352.
36. Madison, D. V., Lipscombe, D., Poenie, M., Reuter, H., Tsien, R. W. & Tsien, R. Y. (1987) *Soc. Neurosci. Abstr.* **13**, 794.
37. Thayer, S. A., Hirning, L. D., Harris, K. M. & Miller, R. J. (1987) *Soc. Neurosci. Abstr.* **13**, 1010.
38. Llinas, R. & Yarom, Y. (1981) *J. Physiol. (London)* **315**, 569–584.
39. Nachshen, D. A. & Blaustein, M. P. (1979) *Mol. Pharmacol.* **16**, 579–586.
40. Reynolds, I. J., Wagner, J. A., Snyder, S. H., Thayer, S. A., Olivera, B. M. & Miller, R. J. (1986) *Proc. Natl. Acad. Sci. USA* **83**, 8804–8807.
41. Obaid, A. L., Flores, R. & Salzberg, B. M. (1987) *Soc. Neurosci. Abstr.* **13**, 99.
42. Turner, T. J. & Goldin, S. M. (1985) *J. Neurosci.* **5**, 841–849.
43. Atchison, W. & O'Leary, S. M. (1987) *Brain Res.* **419**, 315–319.
44. Lemos, J. R. & Nowycky, M. C. (1987) *Soc. Neurosci. Abstr.* **13**, 793.
45. Rane, S. G., Holz, G. G., IV, & Dunlap, K. (1987) *Pflügers Arch.* **409**, 361–366.
46. Rosenbluth, J. (1962) *J. Cell Biol.* **13**, 405–421.
47. Henkart, M., Landis, D. M. D. & Reese, T. S. (1976) *J. Cell Biol.* **70**, 338–347.
48. Cheng, T. P. O. & Reese, T. S. (1987) *J. Neurosci.* **7**, 1752–1759.
49. Watanabe, H. & Burnstock, G. (1976) *J. Neurocytol.* **5**, 125–136.
50. Fujimoto, S., Yamamoto, K., Kuba, K., Morita, K. & Kato, E. (1980) *Brain Res.* **202**, 21–32.